Journal of Organometallic Chemistry, 232 (1982) 171—191
Elsevier Sequoia S.A., Lausanne — Printed in The Netherlands

MOLECULAR ORBITAL ANALYSIS OF THE BONDING IN LOW NUCLEARITY GOLD AND PLATINUM TERTIARY PHOSPHINE COMPLEXES AND THE DEVELOPMENT OF ISOLOBAL ANALOGIES FOR THE $M(PR_3)$ FRAGMENT

DAVID G. EVANS and D. MICHAEL P. MINGOS *

Inorganic Chemistry Laboratory, University of Oxford, South Parks Road, Oxford OX1 3QR (Great Britain)

(Received January 28th, 1982)

Summary

The stoichiometries and geometries of gold and platinum tertiary phosphine cluster compounds of the type $M_n(PR_3)_n^{x+}$ (n = 3—6) have been analysed using extended Hückel molecular orbital calculations. The *isolobal* nature of the $M(PH_3)$ fragment depends critically on the nature of the metal atom M, and may be used to provide a basis for predicting a wide spectrum of homo- and hetero-nuclear metal cluster compounds.

In 1976 we reported a theoretical analysis of the bonding in high nuclearity gold tertiary phosphine cations [1] which provided the basis for the prediction and subsequent successful synthesis of the first example of an icosahedral metal cluster compound [2,3]. This paper describes an extension of this theoretical model to low nuclearity cluster compounds and mixed metal cluster compounds.

The $M(PH_3)$ fragment (M = Ni, Pd, Pt, Cu, Ag, or Au) is a common constituent of the cluster compounds of the platinum and Group Ia metals [4] and has the frontier molecular orbitals represented schematically in Fig. 1a. For these metals the orbitals with a predominance of d orbital character are filled and the bonding characteristics of the fragment are determined primarily by the hy(s-z) and higher lying degenerate pair of metal p_x and p_y orbitals. In terms of *isolobal* analogies [5—7] the $M(PH_3)$ fragment may be identified with either a C—H fragment, which also has a set of hy(s-z), p_x and p_y frontier orbitals, or the conical $M(CO)_3$ fragment, which has the related set of frontier molecular orbitals illustrated in Fig. 1a. Such an analogy based on symmetry considerations ignores possible differences in the bonding capabilities of the fragments arising from the rather different energies and radial characteristics of the orbitals of the central atom. The former is particularly important and Fig. 1b therefore compares the

0022-328X/82/0000—0000/$02.75

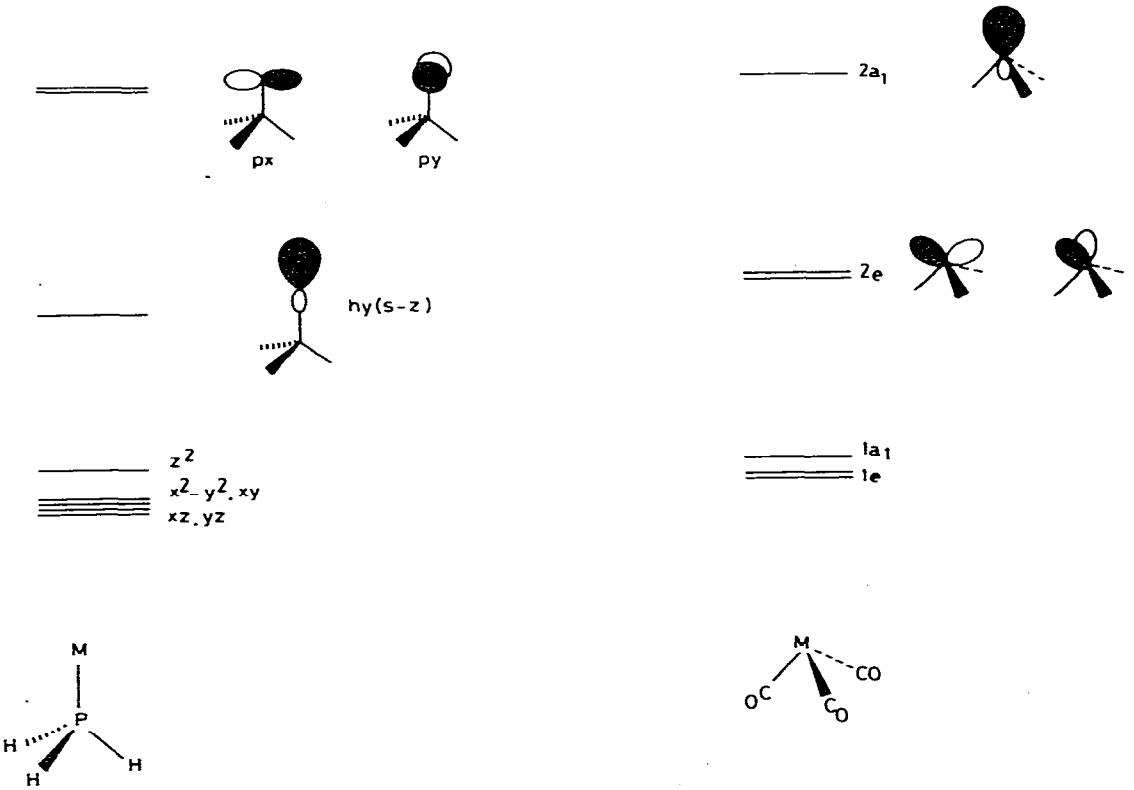

Fig. 1a. A comparison of the frontier molecular orbitals of $M(PH_3)$ and $M(CO)_3$ fragments.

relative energies of the frontier molecular orbitals of $M(PH_3)$ and $M(CO)_3$ [5] fragments as derived from extended Hückel calculations, which are described in further detail in the Appendix. These calculations suggest that although the $M(PH_3)$ fragments, when M = Cu or Ni, may be considered to be *isolobal* with $M(CO)_3$ (M = Cr or Mn) because their frontier orbital energies are approximately the same the analogy is likely to be less reliable for $M(PH_3)$, when M = Au or Pt, because both the hy(*s*-*z*) and p_x, p_y orbitals are significantly less stable than the corresponding orbitals of the $M(CO)_3$ fragments.

From Fig. 1b it is apparent that the following fragments may be considered to a good approximation to be *isolobal* and pseudo-isoelectronic: $Cu(PR_3)$, $Mn(CO)_3$, CH^{2+} and $Ni(PR_3)$, $Cr(CO)_3$, CH^{3+}. This analogy is illustrated by the series of compounds shown in Fig. 1c containing these fragments which are isostructural. The diminished role of the metal p_x and p_y orbitals of the $M(PH_3)$ fragment when M is a third row transition element is demonstrated by the structural determinations on related copper and gold cyclopentadienyl complexes illustrated in Fig. 1d.

In the copper complex [8] the observed η^5-coordination mode maximises the back donation of electron density from filled $e_1(\pi)$ molecular orbitals on the cyclopentadienyl ligand to the empty and relatively low lying p_x, p_y orbitals of the $Cu(PH_3)^+$ fragment. In the case of $Au(PH_3)^+$ the p_x and p_y orbitals are higher

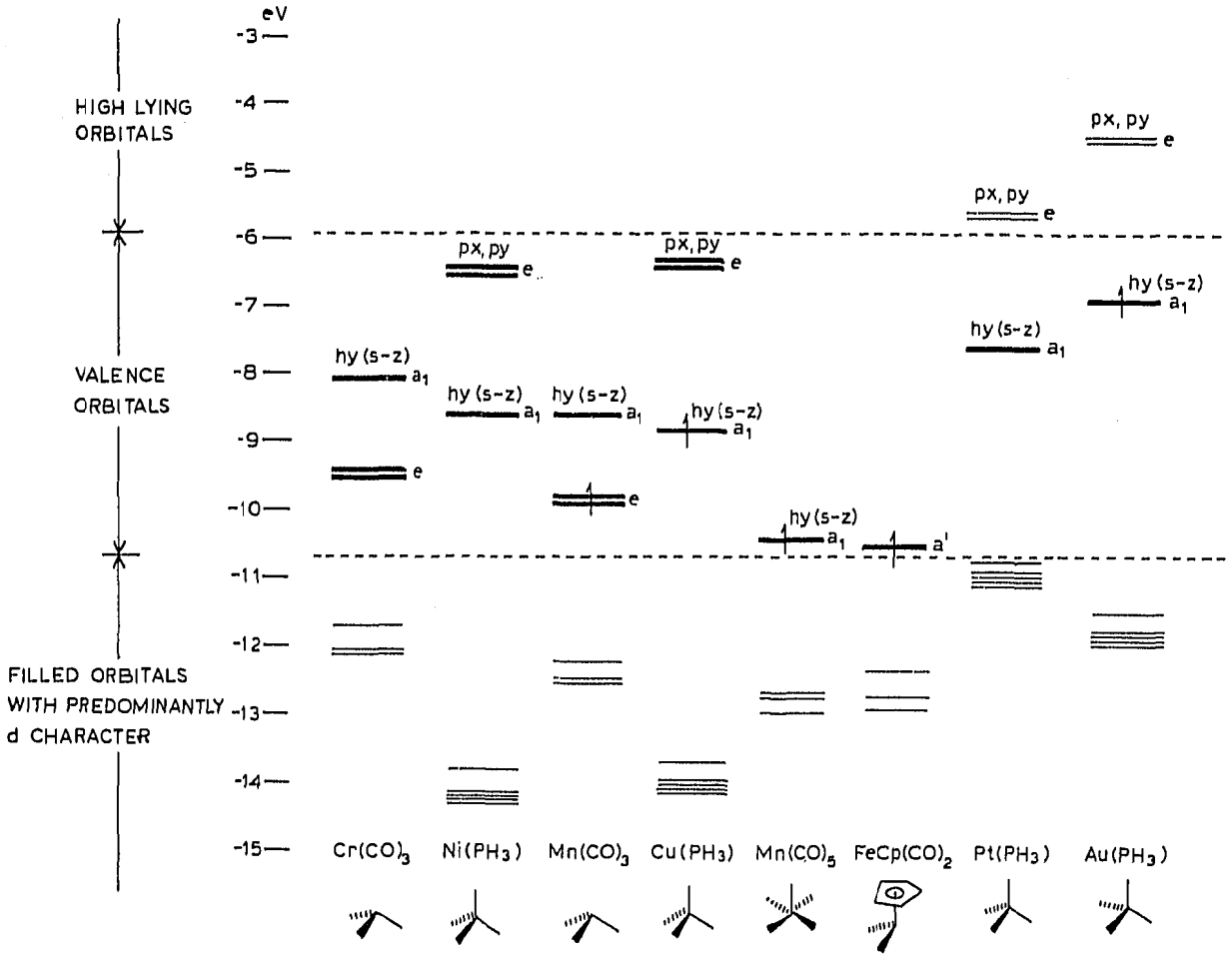

Fig. 1b. A summary of the relative energies of the frontier molecular orbitals of fragments which are *isolobal* with CH, e.g. $Cr(CO)_3$, $Ni(PH_3)$, $Mn(CO)_3$ and $Cu(PH_3)$ and *isolobal* with CH_3 e.g. $Mn(CO)_5$, $FeCp(CO)_2$, $Pt(PH_3)$ and $Au(PH_3)$. The orbitals which lie outside the band marked valence orbitals are not used extensively for bonding.

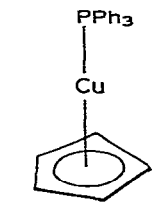

$(C_5H_5)Cu(PPh_3)$
[8]

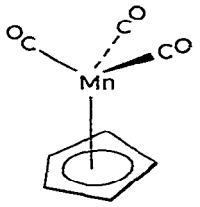

$(C_5H_5)Mn(CO)_3$

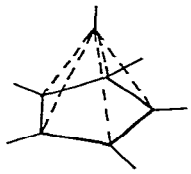

$C_6Me_6^{2+}$
[9]

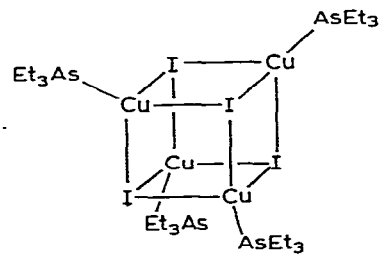

$Cu_4I_4(AsEt_3)_4$
[10]

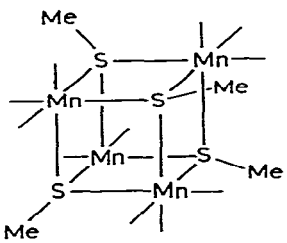

$Mn_4(SMe)_4(CO)_{12}$
[10]

Fig. 1c.

lying and cannot accept this electron density effectively. Consequently, for an η^5-geometry the $e_1(\pi)$molecular orbitals enter into a pair of four electron destabilising interactions with the lower lying and filled metal d_{xz} and d_{yz}

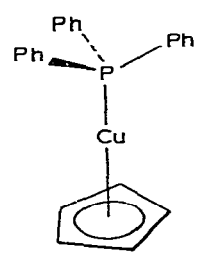

$(C_5H_5)Cu(PPh_3)$
[8]

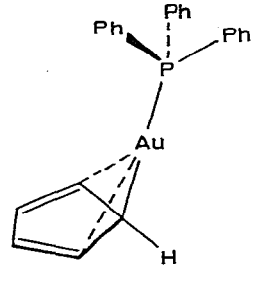

$(C_5HPh_4)Au(PPh_3)$
[11]

Fig. 1d.

orbitals. These destabilising interactions are relieved by a "slip" distortion which leads to a coordination mode intermediate between η^1 and η^3 for the gold atom. The way in which these "slip" distortions reduce the four electron destabilising interactions in such situations has been discussed in some detail by us elsewhere [12]. The extended Hückel calculations which we have completed on these and related systems suggest that the $M(PH_3)$ fragments (M = Au or Pt) approximate to being *isolobal* with CH_3, $Mn(CO)_5$ and $Fe(\eta\text{-}C_5H_5)(CO)_2$ fragments since the p_x and p_y orbitals play only a secondary bonding role. The *isolobal* nature of these fragments has been recognised for some time and is amply demonstrated

by the following series of related molecules: CH_3—CH_3, CH_3—$Au(PPh_3)$, $(OC)_5Mn$—$Mn(CO)_5$ and $(OC)_5Mn$—$Au(PPh_3)$. The *isolobal* nature of $Au(PPh_3)$ and H is more interestingly illustrated by the following pair of cluster compounds [13]:

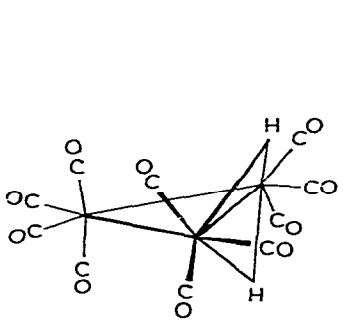

$Os_3H_2(CO)_{10}$

[13a]

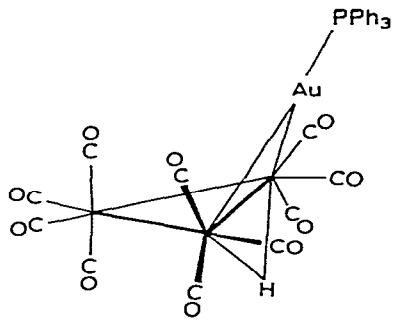

$Os_3H[Au(PPh_3)](CO)_{10}$

[13b]

The high lying nature of the hy(*s*-*z*) orbital of the $Au(PH_3)$ fragment indicated by the calculations and summarised in Fig. 1b, suggests that in complexes of the type $(OC)_5Mn$—$Au(PPh_3)$ the metal—metal bond will be polarised such that the gold atom will bear a positive charge and the manganese atom a negative charge.

The *isolobal* relationships discussed above extend to homonuclear cations derived from these fragments and may be used to account qualitatively for the molecular orbitals of the $[Au_n(PH_3)_n]^{x+}$ cations illustrated in Fig. 2. The symmetries, nodal characteristics and relative energies of the molecular orbitals derived from the hy(*s*-*z*) orbitals of $Au(PH_3)$ fragments are entirely analogous to those of the isostructural H_n^{x+} aggregates [1,14]. From Fig. 2 it is apparent that this analogy is valid because the molecular orbitals derived from the p_x and p_y orbitals of the $Au(PH_3)$ fragments are considerably more higher lying and in general will not make an important contribution to skeletal bonding in this type of unbridged cluster.

The analogy between H and $Au(PR_3)$ fragments leads directly to the important conclusion that the gold—gold bonding interactions in $[Au_n(PR_3)_n]^{x+}$ are maximised for metal polyhedral arrangements based on closed triangles of metal atoms, because these arrangements provide for the maximum number of next neighbour bonding interactions and thereby stabilise most effectively the lowest lying totally symmetric molecular orbital. This generalisation is authenticated by numerous structural studies on gold and platinum cluster compounds containing the $M(PR_3)$ fragment [4]. The molecular orbital calculations which are summarised in Fig. 2 suggest that for low nuclearity clusters the bonding is dominated by the totally symmetric combination of $Au(PH_3)$ hy(*s*-*z*) orbitals and predict the occurrence of the following stable species: $Au_3(PR_3)_3^+$, triangular, 38 valence electrons; $Au_4(PR_3)_4^{2+}$, tetrahedral, 50 valence electrons; $Au_5(PR_3)_5^{3+}$, trigonal, bipyramidal, 62 valence electrons; $Au_6(PR_3)_6^{4+}$, octahedral, 74 valence electrons.

However, the presence of only a single bonding molecular orbital in each of

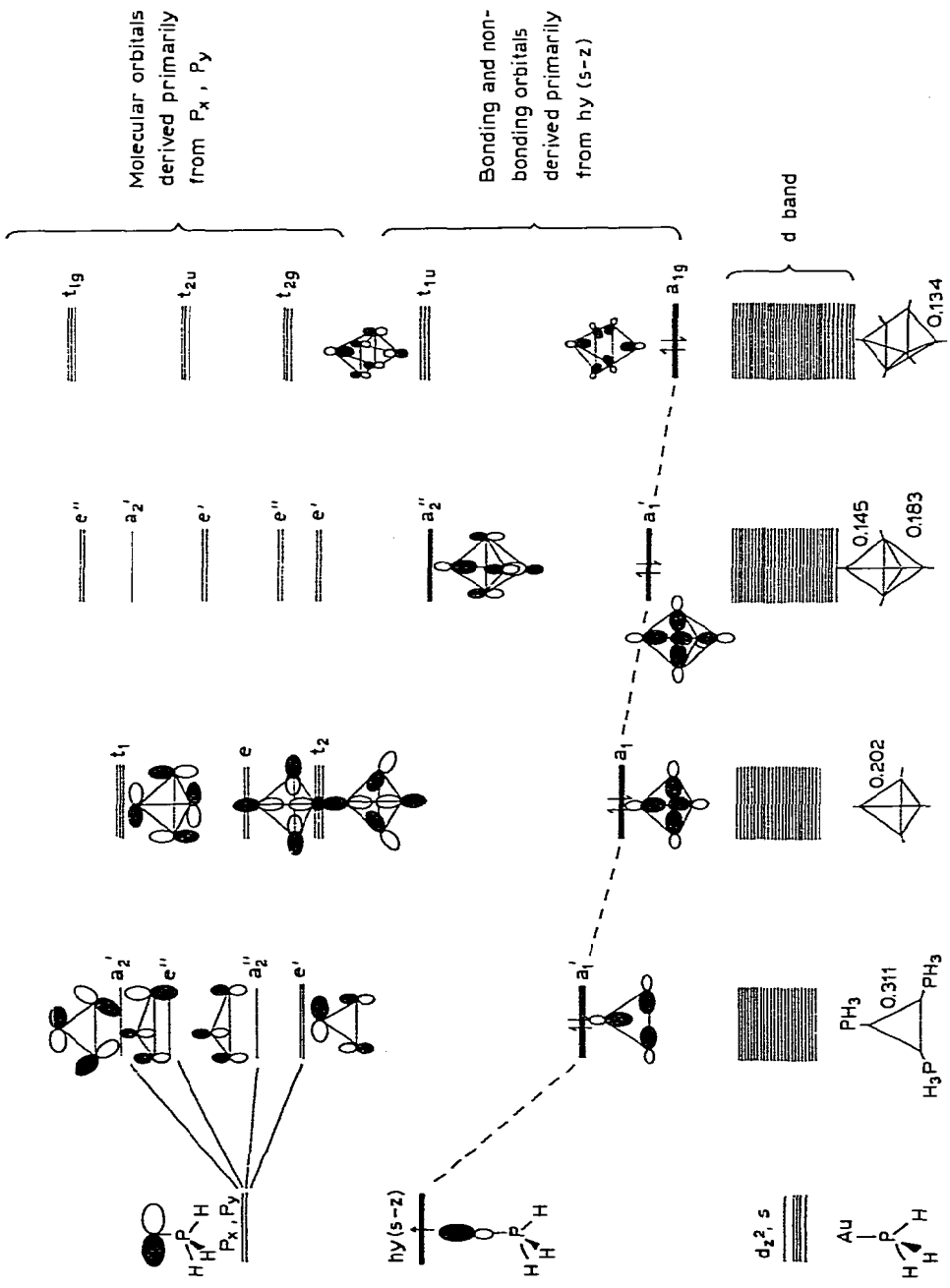

Fig. 2. A summary of the bonding and non-bonding molecular orbitals of $Au_n(PH_3)_n^{x+}$ ($x = n - 2$) with triangular, tetrahedral, trigonal bipyramidal and octahedral geometries. The computed Au—Au overlap populations for these ions are also given at the bottom of the Figure.

these clusters carries with it the implication (confirmed by the Mulliken overlap population analyses reproduced in Fig. 2) of a diminution of gold—gold bonding with increased cluster nuclearity. Therefore the formation of isoelectronic compounds with bridging ligands should enhance the overall stabilities of such compounds. This has been corroborated by extended Hückel molecular orbital calculations on the hydridoclusters $Pt_nH_m(PH_3)_n$, and encouraged by the recent report by Howard, Spencer and their coworkers [15] of the tetrahedral platinum cluster compound $Pt_4H_2(PR_3)_4$, which is isoelectronic with $Au_4(PR_3)_4^{2+}$ discussed above. These calculations also suggest that the bridging ligands could result in the participation of the non-bonding cluster molecular orbitals in Fig. 2 and thereby influence the total electron count. Thus it is possible to predict the occurrence of two platinum octahedral hydridocluster compounds, viz. $Pt_6H_2(PR_3)_6$ and $Pt_6H_8(PR_3)_6$ with the latter arising from the involvement of the non-bonding t_{1u} molecular orbitals of the octahedral cluster shown in Fig. 2. The role of the briding ligands is discussed in more detail below.

Alternative ways of involving the non-bonding t_{1u} molecular orbitals of the octahedral $Au_6(PR_3)_6$ cluster result from distortions of the polyhedron which stabilise preferentially certain components of the t_{1u} set of non-bonding molecular orbitals and thereby improve the gold—gold bonding. Two distortional modes which reduce the symmetry of the octahedron from O_h to either D_{2h} or C_{2v} are illustrated below. The resultant D_{2h} polyhedron may be described in terms of two tetrahedra which have been fused along a common edge. The C_{2v} polyhedron may alternatively be described as a bicapped tetrahedron. These polyhedra are closely related and the bicapped tetrahedron may be generated from the fused tetrahedra by the formation of an additional bond between non-adjacent vertices of the tetrahedra.

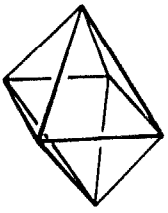

OCTAHEDRON

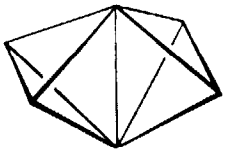

EDGE SHARING TETRAHEDRA

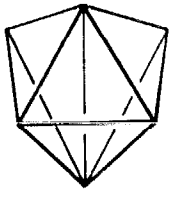

BICAPPED TETRAHEDRON

The effects of such distortions on the frontier molecular orbitals of the octahedral $Au_6(PH_3)_6$ cluster are illustrated in Fig. 3a and 3b. In each case the lowest lying a_{1g} molecular orbital is essentially unaffected, but the t_{1u} set of molecular

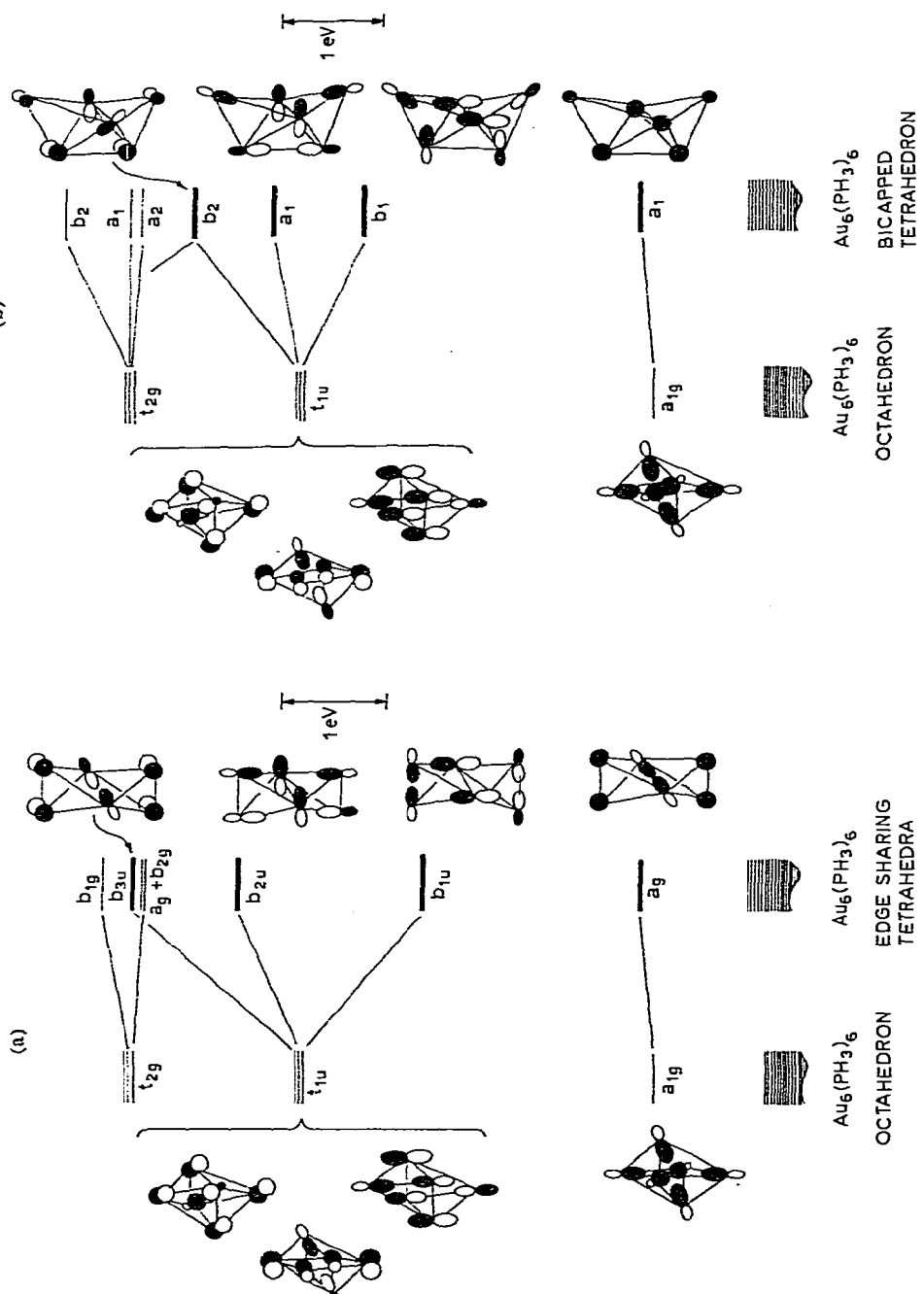

Fig. 3. The effect on the frontier molecular orbitals of the octahedral $Au_6(PH_3)_6$ cluster of condensing the structure to a fused edge sharing tetrahedral situation (Fig. 3a) and a bicapped tetrahedron (Fig. 3b). Particularly noteworthy is the stabilisation of the $^b1(u)$ components of the t_{1u} set.

orbitals is split into three components with dramatically different energies. For the D_{2h} fused tetrahedra the b_{1u} component is stabilised by approximately 1 eV, the b_{2u} component is destabilised by approximately 0.5 eV and the b_{3u} component is destabilised by more than 1.5 eV. These energy changes can readily be understood in terms of the changes in overlap integrals between the orbitals on adjacent atoms, which accompany the polyhedral transformation from octahedral to fused tetrahedral. These changes are represented in a schematic fashion in Fig. 3a. For the bicapped tetrahedron the b_1 component of the t_{1u} set of octahedral molecular orbitals (see Fig. 3b) is stabilised by only 0.6 eV, the a_1 component is slightly destabilised (0.2 eV) and the b_2 component is destabilised by 1.0 eV. Therefore, qualitatively the removal of the degeneracy of the t_{1u} set is similar for the fused tetrahedra and the bicapped tetrahedron, but the magnitudes of the splittings are larger in the former case. This difference can be easily understood by comparing the nodal characteristics of the b_{1u} and b_1 components of the t_{1u} set in Fig. 3a and 3b respectively. The latter has an additional out-of-phase overlap between the gold 6*p* orbitals across the additional edge of the bicapped tetrahedron.

It follows from the Walsh diagrams in Fig. 3a and 3b that the bicapped tetrahedral and fused tetrahedral structures are most effectively stabilised compared to the parent octahedral structure when the a_1 and b_1 (or a_g and b_{1u}) components are simultaneously occupied by electron pairs, i.e. for the stoichiometry $[Au_6(PH_3)_6]^{2+}$. It also follows from the theoretical analysis presented in Fig. 3a and 3b that for such an ion the preferred geometry is fused tetrahedral rather than bicapped tetrahedral. This conclusion follows directly from the greater stabilisation of the b_{1u} component in the former case than the b_1 component in the latter. This conclusion provides an interesting comparison with osmium carbonyl chemistry where for example in $Os_6(CO)_{18}$ the bicapped tetrahedral geometry is preferred.

The computed total energies for the $Au_6(PH_3)_6^{x+}$ polyhedra summarised in Table 1 suggest that the fused tetrahedral geometry is also preferred for the neutral $Au_6(PH_3)_6$ molecule, but the margin of stability compared to the octahedron and bicapped tetrahedron is much smaller. The reasons for this lie in the higher energy of the b_{2u} component in Fig. 3a. For the $Au_6(PH_3)_6^{4+}$ ion the octahedral geometry is the most stable, but the energy differences separating the alternative geometries is so small that such an ion might be stereochemically non-rigid.

Interestingly, Bour et al. [16] have recently reported the characterisation of $Au_6(PPh_3)_4\{Co(CO)_4\}_2$, which is isoelectronic with $Au_6(PR_3)_6^{2+}$, and demonstrated that it has the fused tetrahedral structure described above. The com-

TABLE 1

SUM OF THE ONE ELECTRON ORBITAL ENERGIES FOR $Au_6(PH_3)_6^{x+}$ (eV)

	$Au_6(PH_3)_6^{4+}$	$Au_6(PH_3)_6^{2+}$	$Au_6(PH_3)_6$
Octahedron	−1592.3	−1605.8	−1619.4
Bicapped tetrahedron	−1592.1	−1606.8	−1619.9
Fused tetrahedra	−1592.0	−1607.8	−1620.2

puted overlap populations for the $Au_6(PH_3)_6^{2+}$ ion which are reproduced in the figure below demonstrate clearly the bonding advantage gained in terms of metal—metal bonding compared to the related $Au_6(PH_3)_6^{4+}$ ion with an octahedral geometry, where the Au—Au overlap population is computed to be only 0.134. Qualitatively, the preference for a fused tetrahedral structure can be appreciated in terms of forming two tetrahedral entities each with a totally symmetric and filled bonding molecular orbital rather than the parent octahedral structure which has only a single in phase bonding molecular orbital.

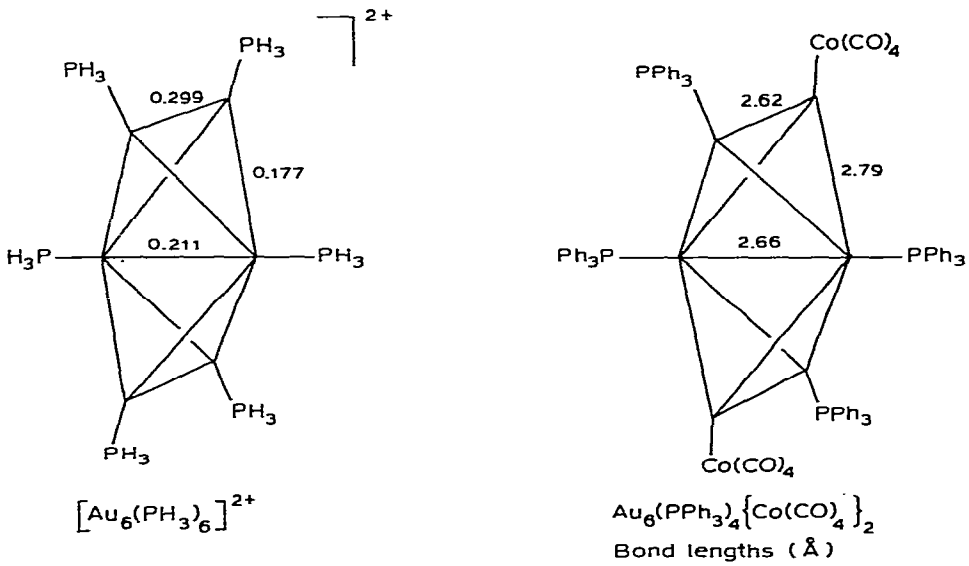

$[Au_6(PH_3)_6]^{2+}$

$Au_6(PPh_3)_4\{Co(CO)_4\}_2$

The trends in the computed overlap populations reproduced above account nicely for the range of metal—metal bond lengths reported for $Au_6(PPh_3)_4\{Co(CO)_4\}_2$ [16] and summarised above. The computed overlap populations and bond lengths given above reflect the nodal characteristics of the highest occupied molecular orbital, b_{1u} in Fig. 3a. This molecular orbital is localised extensively on the three edges of the fused tetrahedra which are bisected by the major two-fold axis of the ion. Furthermore, it is strongly σ-bonding along the outer two edges and π-bonding along the common edge of the fused tetrahedra (see Fig. 3a). This type of asymmetry in bonding readily accounts for the observed trends in overlap populations.

There has been a report of an octahedral cluster with the stoichiometry $Au_6(PPh_3)_6^{2+}$, which as we have pointed out previously does not conform to the bonding ideas developed above [1]. Since this compound was only prepared in very small quantities and characterised by means only of a single crystal X-ray analysis [17] these calculations reinforce the doubts expressed previously concerning the charge on this cation.

The *isolobal* nature of $Au(PR_3)$ and the $M(CO)_5$ fragment as illustrated in Fig. 1b may be used profitably in conjunction with the cluster molecular orbital calculations described above to predict the occurrence of the following series of tetrahedral and triangular mixed metal compounds, which have a single skeletal electron pair.

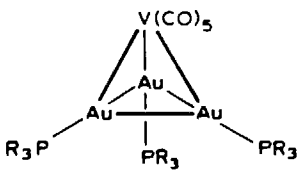

$Au_3(PR_3)_3V(CO)_5$

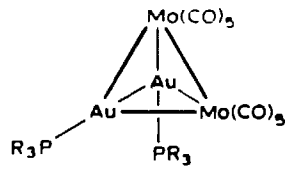

$Au_2(PR_3)_2Mo_2(CO)_{10}$

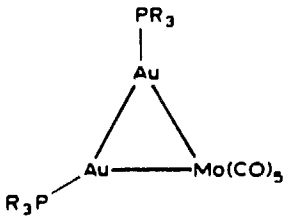

$Au_2(PR_3)_2Mo(CO)_5$

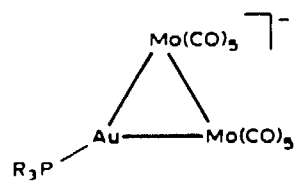

$[Au(PR_3)Mo_2(CO)_{10}]^-$

The synthesis and structural characterisation of the complex $(OC)_5VAu_3(PPh_3)_3$ has been reported recently and the compound shown to have the tetrahedral structure illustrated above, rather than the alternative 8-coordinate vanadium(III) compound which would have been predicted on the basis of simple valency considerations [18].

The secondary bonding role of the p_x and p_y orbitals of the $Au(PH_3)$ fragment discussed above in the context of the polyhedral transformation from octahedral to fused tetrahedral, is also discernible in tetrahedral clusters of these fragments with bridging ligands. The utilization of these orbitals is particularly important for understanding why in closely related tetrahedral cluster compounds of the type $M_4(PR_3)_4X_2$, where X is a monoanionic bridging ligand, the total electron count can vary from 50, for example in $Pt_4H_2(PR_3)_4$ [14], to 54, for example in $Au_4I_2(PPh_3)_4$ [19].

The structure of $Pt_4H_2(PBu^t)_4$ reported by Howard, Spencer and their coworkers [15] involves a Pt_4P_4 core which deviates only slightly from T_d symmetry, which implies that the hydride ligands occupy bridging rather than terminal coordination sites, but the hydride ligands were not located. In the calculations described here the hydride ligands have been located on opposite edges of the metal tetrahedron, thereby effectively lowering the symmetry to D_{2d}.

Figure 4 illustrates the interaction diagram for the platinum cluster compound $Pt_4H_2(PH_3)_4$ with the bridged geometry described above. The a_1 and b_2 combinations of the hydrogen 1s orbitals interact primarily with cluster molecular orbitals with matching symmetries derived from the d band. The resultant interaction diagram thereby maintains the electron count predicted for the unbridged tetrahedron, i.e. $Pt_4(PR_3)_4^{2+}$, which has molecular orbitals similar to those illustrated in Fig. 2 for the isoelectronic gold compound.

Hydrido complexes of gold are not particularly stable and consequently within the province of gold cluster chemistry the cluster compounds are stabilised by alternative bridging groups. The location of ligands such as I^- along the same

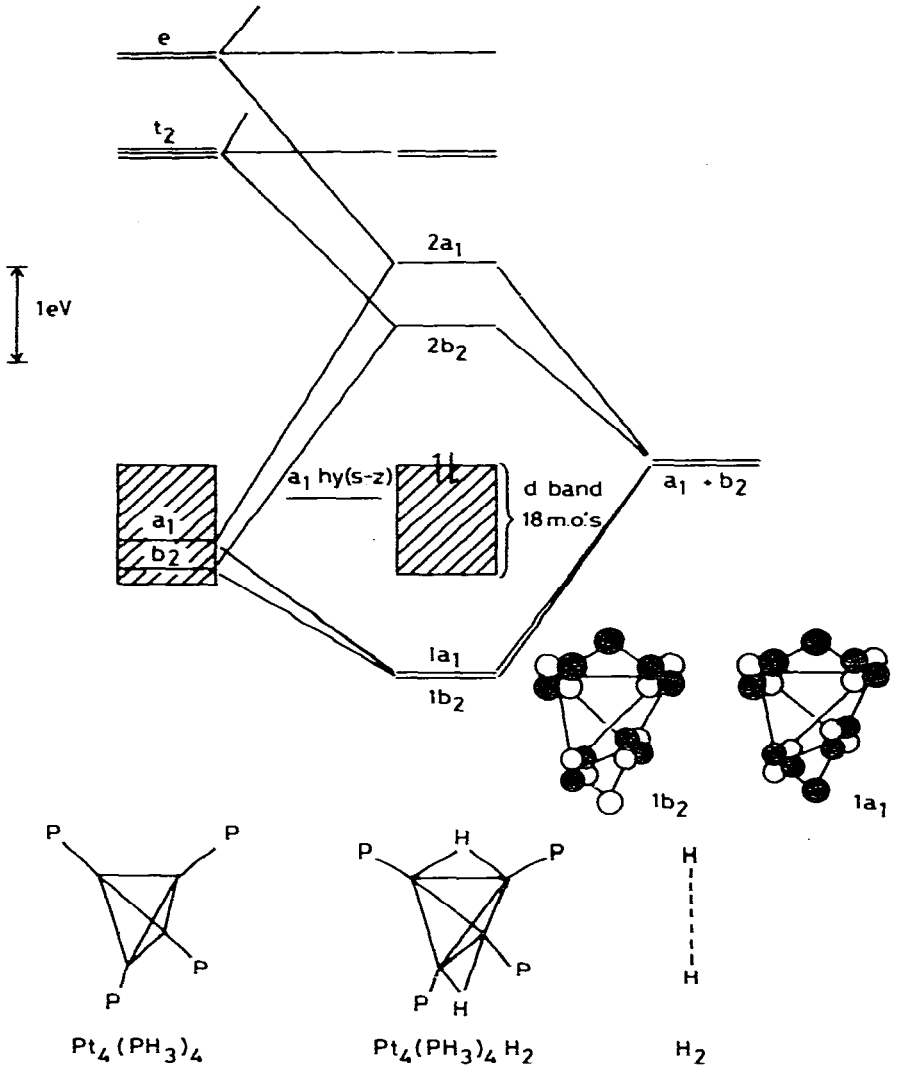

Fig. 4. Interaction diagram for the formation of the edge bridged hydrido- cluster compound $Pt_4H_2(PH_3)_4$. For the parent $Pt_4(PH_3)_4$ cluster the a_1 molecular orbital derived from hy(*s-z*) is more stable than the comparable orbital in the gold complex and lies within the *d* band of molecular orbitals. It interacts little with the hydrogen 1*s* orbitals of the bridging hydrido- ligands. In $Pt_4(PH_3)_4H_2$ the electronic configuration is $(1b_2)^2(1a_1)^2(d\text{-band})^{36}(a_1\text{-hy}(s\text{-}z))^2$, i.e. a total of 50 valence electrons if the Pt—P bonding molecular orbitals are included.

edges as those occupied by the hydrido- ligands in the cluster above requires the D_{2d} distortion of the Au_4P_4 skeleton illustrated below. For the calculations described in this paper the phosphine ligands were distorted in this fashion until the Au—Au—P bond angle was equal to 180°.

This distortion has the effect of raising the energy of the totally symmetric combination of molecular orbitals derived from hy(*s-z*) of the isolated $Au(PH_3)$ fragments. The distortion also raises the degeneracies of the higher lying t_2 and *e* molecular orbitals. The b_2 component of the t_2 set is stabilised by a large

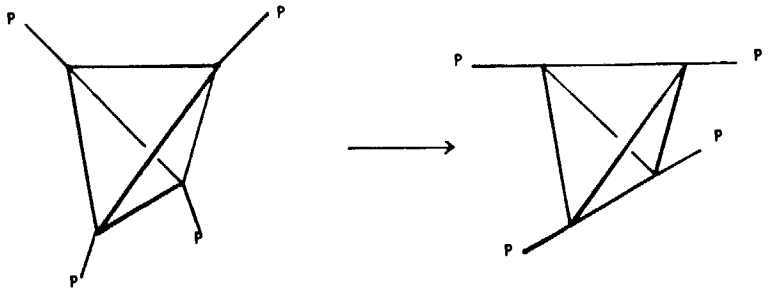

amount and the e component destabilised. The changes in interatomic overlap integral which give rise to the observed energy changes are illustrated schematically in Fig. 5. The b_2 component is bonding along those edges of the tetrahedron which are intersected by the S_4 axis and has the appropriate radial characteristics to interact effectively with the donor orbitals of bridging ligands located along these edges. The importance of the D_{2d} distortion in stabilising the $Au_4I_2(PH_3)_4$ structure is underlined by calculations on this molecule with Au—Au—P equal to 145 and 180°. The structure with this angle equal to 180° was found to be 2.8 eV more stable than the undistorted structure. In part this difference can be attributed to steric effects (within the context of this type of calculation four electron destabilising interactions between the filled orbitals of the iodine and phosphorus and hydrogen atoms), but approximately 25% of the energy difference can be attributed to electronic effects originating primarily from the stabilisation of the b_2 component of the t_2 set.

Figure 6 illustrates the interaction diagram for the $Au_4(PH_3)_4$ moiety with a D_{2d} distorted geometry and two iodide ligands located in bridging positions along the S_4 axis. The a_1 combination of iodide lone pair orbitals interact primarily with the cluster a_1 bonding molecular orbital derived from hy(s-z), and the b_2 combination with the b_2 cluster molecular orbital derived from the t_2 set in the undistorted structure. The bonding components which result from these interactions, $1a_1$ and $1b_2$ in Fig. 6, are localised predominantly on the iodide ligands. Simple frontier orbital ideas would suggest that the most stable electronic situation for the $Au_4I_2(PH_3)_4$ species would result from the occupation of the bonding $1a_1$ and $1b_2$ molecular orbitals, i.e. for the $Au_4I_2(PH_3)_4^{2+}$

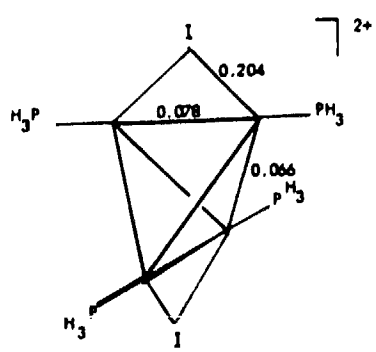

$[Au_4I_2(PH_3)_4]^{2+}$

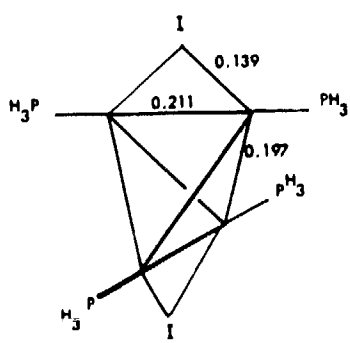

$Au_4I_2(PH_3)_4$

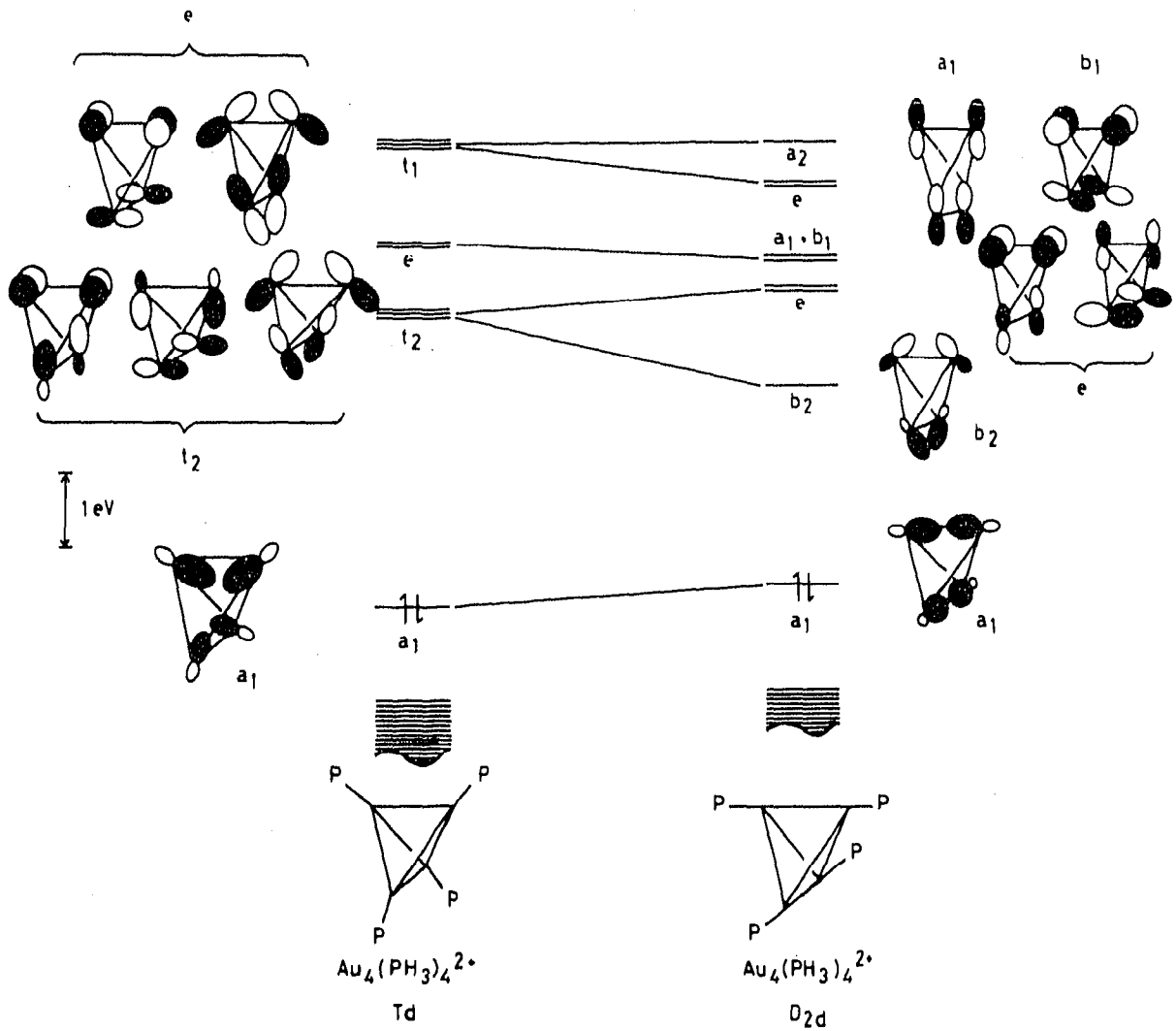

Fig. 5. An illustration of the effect of increasing the Au—Au—P bond angles to 180°, whilst maintaining D_{2d} symmetry, on the frontier molecular orbitals of the tetrahedral $Au_4(PH_3)_4$ cluster. Particularly noteworthy is the stabilisation of the b_2 component of the t_2 set.

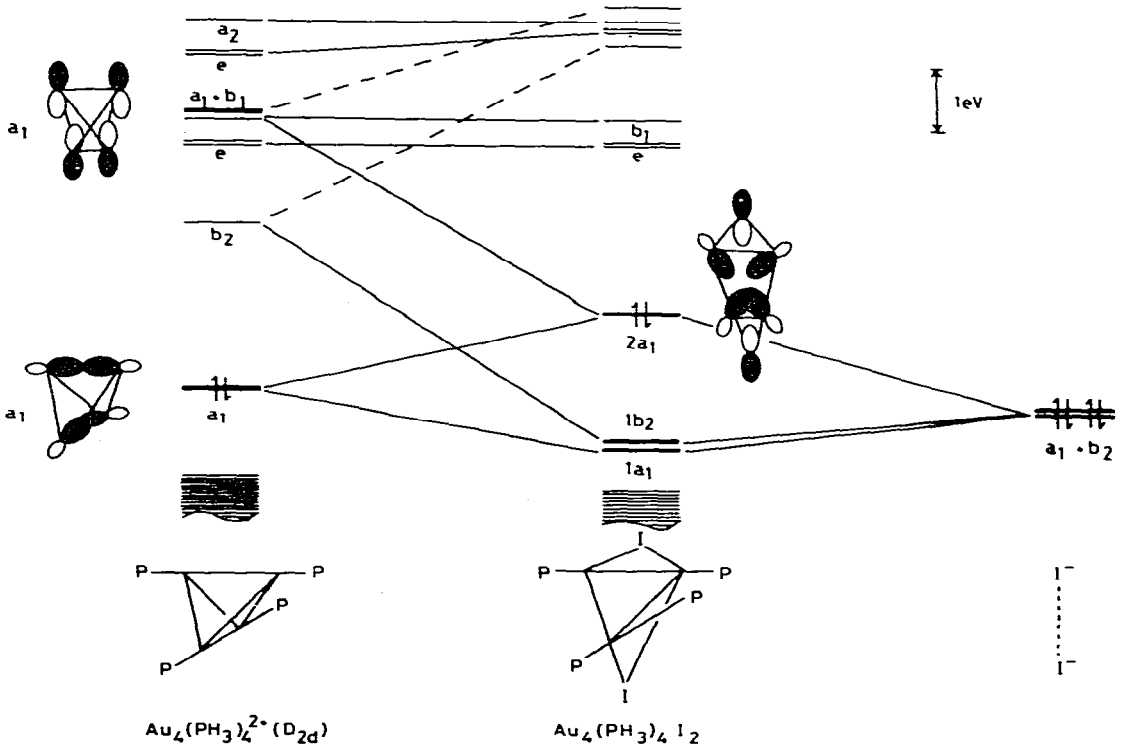

Fig. 6. Illustration of the orbital interactions between $Au_4(PH_3)_4$ and the frontier molecular orbitals of the bridging iodide ligands. The highest occupied molecular orbital in $Au_4I_2(PH_3)_2$ is $2a_1$. This leads to a total electron count of 54 if the iodides are viewed as 1 electron bridging ligands.

cation. However, the overlap populations computed for such an ion and reproduced above suggest that there is little effective gold—gold bonding in such an ion. This results because the $1a_1$ and $1b_2$ molecular orbitals are so intensively localised on the iodide ligands that little bonding electron density remains between the gold atoms.

The situation is improved significantly by the population of the higher lying $2a_1$ molecular orbital in Fig. 6. The computed overlap populations for the resultant neutral molecule, $Au_4I_2(PH_3)_4$, summarised above indicate that the additional electron pair resides in a molecular orbital which is considerably more bonding between the gold atoms and only slightly antibonding between gold and iodide. The fact that this molecular orbital is not strongly gold—iodide antibonding is at first sight surprising since this molecular orbital may be identified as the antibonding partner to $1a_1$ in Fig. 6. However, the antibonding character of $2a_1$ is significantly diminished by a contribution from the higher lying and empty cluster molecular orbital of a_1 symmetry derived from the e set of the undistorted tetrahedron (see Fig. 5 and 6). The manner by which this mixing diminishes the antibonding gold—iodide character of the $2a_1$ molecular orbital is illustrated schematically overleaf.

At the same time population of this orbital leads to a substantial strengthening of the gold—gold bonding within the tetrahedron. Therefore the calculations

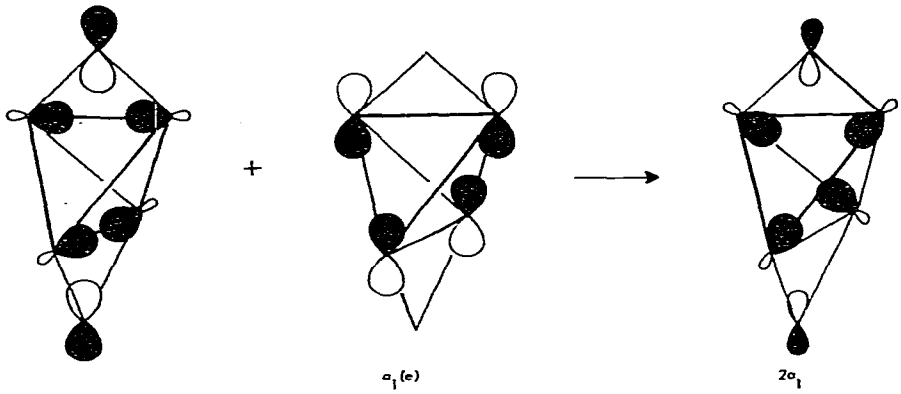

suggest that the neutral gold cluster $Au_4I_2(PR_3)_4$ with 54 valence electrons is the more stable cluster species.

Such a molecule has recently been synthesised and structurally characterised by Manaserro, Naldini and Sansoni [19], who noted that the Au—Au bond lengths in the cluster were shorter for those edges bridged by iodide than the remaining four edges. The nature of this structural asymmetry is clearly indicated in the figure below.

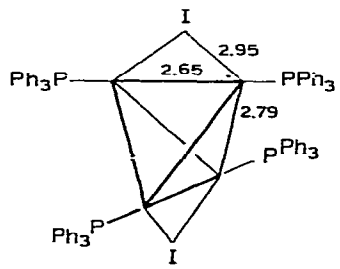

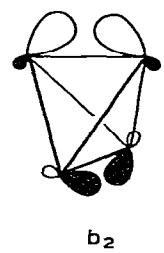

$Au_4I_2(PPh_3)_4$ – Bond lengths (Å)

The calculations which we have completed on this molecule suggest that this asymmetry can be attributed primarily to the bonding contribution of the cluster b_2 molecular orbital, which is more strongly bonding along the two bridged edges (see Fig. 5 and 6). The computed overlap populations which reproduce this trend are summarised on p. 191.

In $Au_4I_2(PH_3)_4$, which has a total of 54 valence electrons, the ligand a_1 combination enters into a 3 orbital 4 electron interaction with the cluster a_1 molecular orbitals derived from hy(s-z) and the e set. This situation is possible because the middle component of such an interaction ($2a_1$ in Fig. 6) is reasonably low lying, non-bonding with respect to the bridging ligands, and bonding with respect to the cluster. If the energies of the a_1 and b_2 combinations of the ligand orbitals match those of the cluster skeletal molecular orbitals more closely then the situation alters dramatically and the a_1 orbitals enter into a two electron three orbital interaction, rather than a four electron three orbital interaction. The reasons for this can be clearly appreciated from Fig. 7 which illustrates the effect of bridging the tetrahedral cluster with two angular $Au(PH_3)_2$ fragments in the following fashion:

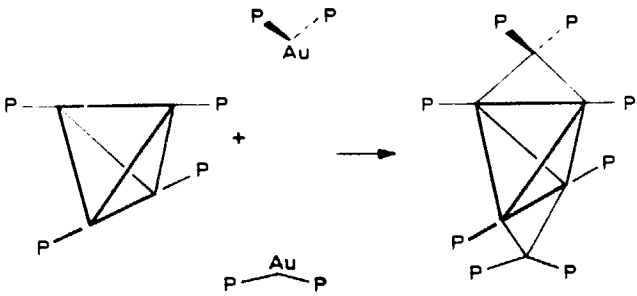

The frontier molecular orbitals of the $M(PH_3)_2$ fragment, which have been discussed in some detail by us previously [12,20], are reproduced in Fig. 7. From the point of view of the present bonding analysis the important feature of this fragment arises from the fact that the odd electron resides in the highest occupied molecular orbital which is a hybrid hy(*s*-*z*) orbital similar to that described above for $Au(PH_3)$. It also resembles the lone pair orbital of the bridging iodide ligand.

Figure 7, which illustrates the important interactions in the $Au_4(PH_3)_4\{\mu\text{-}Au(PH_3)_2\}_2$ cluster, suggests that the a_1 and b_2 combinations derived from this molecular orbital are higher lying than the bonding a_1 cluster molecular orbital derived from hy(*s*-*z*) of the isolated $Au(PH_3)$ fragments. Therefore, the bonding molecular orbitals derived from the in phase combination of a_1 orbitals ($1a_1$ in Fig. 7) is localised predominantly on the tetrahedral cluster. The energy match between the b_2 molecular orbitals is good and therefore the bonding $1b_2$ molecular orbital is strongly bonding between cluster and bridging gold atoms. The occupation of $1a_1$ and $1b_2$ in Fig. 7 therefore leads to effective bonding between all six gold atoms and diminishes the necessity of occupying the $2a_1$ molecular orbital, which is much higher lying than the corresponding molecular orbital in $Au_4I_2(PH_3)_4$ illustrated in Fig. 6. The $1a_1$, $1b_2$ and $2a_1$ molecular orbitals of $Au_4(PH_3)_4\{\mu\text{-}Au(PH_3)_2\}_2$ are illustrated schematically in Fig. 8.

If the $Au(PH_3)_2$ fragments are viewed as 1 electron bridging ligands then the occupation of $1a_1$ and $1b_2$ corresponds to a total electron count of 52 valence electrons, i.e. the stoichiometry $[Au_6(PH_3)_8]^{2+}$.

The computed overlap populations for $Au_4(PH_3)_4\{\mu\text{-}Au(PH_3)_2\}_2^{2+}$ summarised below suggest that the degree of asymmetry in cluster bonding should be more pronounced in this type of cluster than that noted above for $Au_4I_2(PH_3)_4$. This conclusion results from the b_2 molecular orbital being more localised on the tetrahedral cluster in the former case.

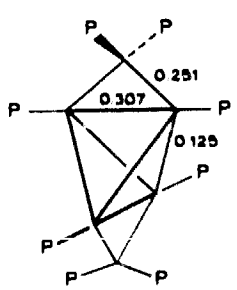

Overlap populations

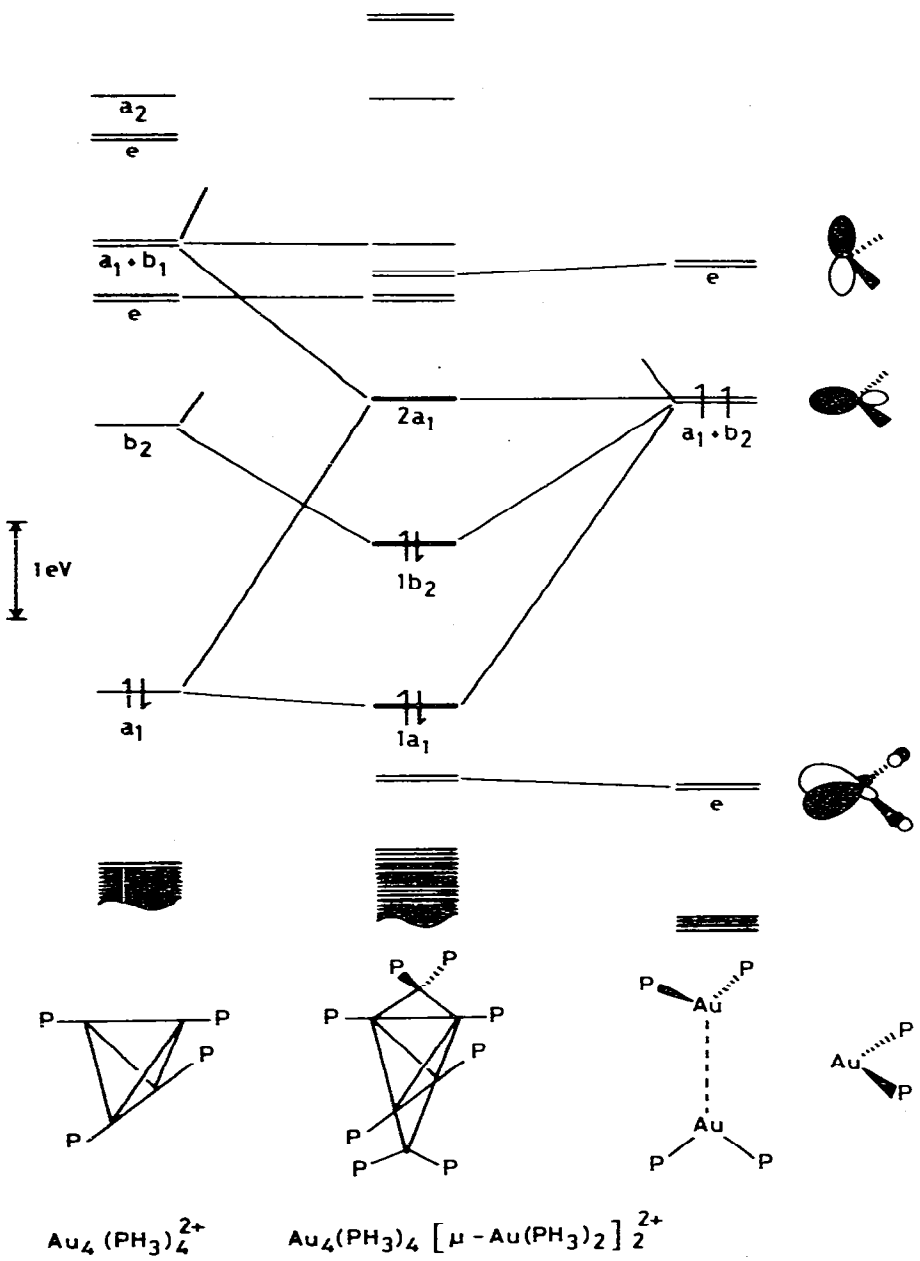

Fig. 7. Illustration of the orbital interactions between $Au_4(PH_3)_4$ and two edge bridging $Au(PH_3)_2$ ligands. The highest occupied molecular orbital is $1b_2$.

Although this analysis has been undertaken for the $Au(PH_3)_2$ fragment as a bridging ligand in order to get the most suitable match in cluster and bridging ligand orbitals similar arguments are relevant to other fragments which are *isolobal* with $Au(PH_3)_2$, e.g. $Mn(CO)_5$ and $Co(CO)_4$. The $Au(PH_3)$ fragment could also be viewed as being *isolobal* with $Au(PH_3)_2$ and therefore it could be

argued that it could function in a similar fashion leading to an isostructural derivative of stoichiometry $Au_6(PH_3)_6^{2+}$. This structure therefore provides an alternative geometry to the fused tetrahedral and bicapped tetrahedral structures discussed previously for $Au_6(PH_3)_6^{2+}$. Indeed calculations for this stoichiometry have shown that the fused tetrahedral and edge bridged tetrahedral struc-

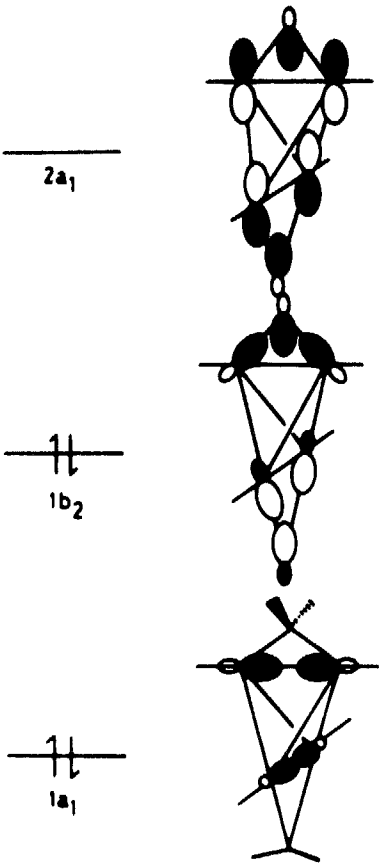

Fig. 8. Schematic illustration of the frontier molecular orbitals of $Au_4(PH_3)_4\{\mu\text{-}Au(PH_3)_2\}_2$. It is the nodal characteristics of the $1b_2$ molecular orbital which leads to the observed asymmetry in computed overlap populations.

tures of $Au_6(PH_3)_6^{2+}$ have almost identical energies. Close inspection of the charge distributions and overlap populations for the two alternative structures have failed to indicate good reasons for the adoption of the fused tetrahedral structure in the case of $Au_6(PPh_3)_4\{Co(CO)_4\}_2$ [30].

Conclusion

Although to a first approximation the $Au(PH_3)$ fragment can be considered to be *isolobal* with fragments such as CH_3, $Mn(CO)_5$ and $Co(CO)_4$ which have only a single frontier orbital available for bonding it is necessary to also take

into account the secondary contribution made by the $6p_x$ and $6p_y$ orbitals of gold in order to satisfactorily account for the stoichiometries and bond lengths of small gold cluster compounds derived from this fragment. Condensed polyhedral structures based on the tetrahedron appear to be particularly favourable for small gold phosphine cluster compounds, because they provide for the maximum number of nearest neighbour gold—gold interactions and a pair of bonding cluster molecular orbitals derived from the hy(s-z) orbitals of the isolated Au(PH_3) fragment.

Acknowledgement

The S.E.R.C. is thanked for their financial support, and Mrs Christine Palmer for her assistance with the Figures.

Appendix

All the calculations were performed using the extended Hückel method [21,22] and the relevant orbital parameters are given in the Tables below.

The H_{ii} for the bridging hydrido ligands were set equal to −10.0 eV rather than the usual value of −13.60 eV in order to model more effectively the hydridic nature of these ligands [24]. The conclusions reached in the paper are not altered when the usual H_{ii} is used, but the resultant charge distributions conform more closely to electroneutrality when the lower values are used.

TABLE 1A

PARAMETERS FOR NON-METAL ATOMS

Atom	Orbital	Slater exponent	H_{ii} (eV)	ref.
H	1s(in PH_3)	1.30	−13.60	21
H	1s(Bridging)	1.30	−10.00	24
P	3s	1.60	−18.60	25
	3p	1.60	−14.00	25
I	5s	2.63	−22.30	26
	5p	2.20	−11.00	26

TABLE 2A

PARAMETERS FOR METAL ATOMS

Atom	Orbital	H_{ii} (eV)	ξ_1	c_1	ξ_2	c_2	ref.
Pt	6s	−9.80	2.55				27
	6p	−5.35	2.55				27
	5d	−10.61	6.01	0.633	2.70	0.551	27
Au	6s	−9.22	2.60				1
	6p	−4.27	2.58				1
	5d	−11.85	6.16	0.648	2.73	0.539	1

All the parameters conform to those which have been used to give reliable conclusions for organo-transition metal compounds [6,28]. The off diagonal terms in the extended Hückel calculations were estimated from the expression $H_{ij} = 1.75S_{ij}(H_{ii} + H_{jj})/2$ [21,29].

The following bond lengths were used for the calculations: Au—Au 2.70 Å, Pt—Pt 2.70 Å, Au—P 2.27 Å, Pt—P 2.27 Å, Au—I 2.90 Å, Pt—H 1.80 Å, P—H 1.42 Å. The calculations were performed on the ICL 2980 Computer at this University using the programs ICON8 and FMO [22].

References

1 D.M.P. Mingos, J. Chem. Soc. Dalton, (1976) 1163.
2 C.E. Briant, B.R.C. Theobald, J.W. White, L.K. Bell, A.J. Welch and D.M.P. Mingos, J. Chem. Soc. Chem. Commun., (1981) 201.
3 D.M.P. Mingos, Pure Appl. Chem., 52 (1980) 705.
4 P.R. Raithby in B.F.G. Johnson (Ed.), Transition Metal Clusters, Wiley, Chichester, 1980, p5.
5 M. Elian, M.M.L. Chen, R. Hoffmann and D.M.P. Mingos, Inorg. Chem., 15 (1976) 1148.
6 D.M.P. Mingos, Adv. Organometal. Chem., 15 (1977) 1.
7 M.I. Forsyth and D.M.P. Mingos, J. Chem. Soc. Dalton, (1977) 610.
8 F.A. Cotton and J. Takats, J. Amer. Chem. Soc., 92 (1970) 2353.
9 H. Hogeveen and P.W. Kwant, J. Amer. Chem. Soc., 96 (1974) 2208.
10 C.D. Garner in B.F.G. Johnson and J. Wiley (Eds.), Transition Metal Clusters, Chichester, 1980, p265.
11 T.V. Baukova, Yu.L. Slovakhotov, Yu.T. Struchkov, J. Organometal. Chem., 220 (1981) 125.
12 M.I. Forsyth, D.M.P. Mingos and A.J. Welch, J. Chem. Soc. Dalton, (1978) 1363, and ref. therein.
13 A.G. Orpen, A.V. Rivera, E.G. Bryan, D. Pippard, G. Sheldrick and K.D. Rouse, J. Chem. Soc. Chem. Commun., (1978) 723; B.F.G. Johnson, D.A. Kaner, J. Lewis and P.R. Raithby, J. Organometal. Chem., 215 (1981) C33.
14 A.J. Stone, Inorg. Chem., 20 (1981) 563; S.W. Harrison, L.J. Massa and P. Solomon, Nature (Phys. Science), 245 (1973) 31.
15 P.W. Frost, J.A.K. Howard, J.L. Spencer and D.G. Turner, J. Chem. Soc. Chem. Commun., (1981) 1104.
16 J.W.A. Van der Welden, J.J. Bour, B.F. Otterloo, W.P. Bosman and J.H. Noordik, J. Chem. Soc. Chem. Commun., (1981) 583.
17 P.L. Bellon, M. Manasserro and M. Sansoni, J. Chem. Soc. Dalton, (1973) 2423.
18 J.E. Ellis, J. Amer. Chem. Soc., 103 (1981) 6106.
19 F. Demartin, M. Manasserro, L. Naldini, R. Ruggeri and M. Sansoni, J. Chem. Soc. Chem. Commun., (1981) 222.
20 D.M.P. Mingos, J. Chem. Soc. Dalton, (1977) 602; A. Dedieu and R. Hoffmann, J. Amer. Chem. Soc., 100 (1978) 2074.
21 R. Hoffmann, J. Chem. Phys., 39 (1963) 1397.
22 J. Howell, A. Rossi, D. Wallace, K. Haraki and R. Hoffmann, Quantum Chemistry Program Exchange, 10 (1977) 344.
23 J.W. Richardson, W.C. Nieuwpoort, R.R. Powell and W.F. Edgell, J. Chem. Phys., 36 (1962) 1057.
24 R. Hoffmann, B.E.R. Schilling, R. Bau, H.D. Kaesz and D.M.P. Mingos, J. Amer. Chem. Soc., 100 (1978) 6088.
25 E. Clementi, J. Chem. Phys., 40 (1964) 1944.
26 P. Pyykkö and L.L. Lohr Jr., Inorg. Chem., 20 (1981) 1950.
27 F.A. Cotton and C.B. Harris, Inorg. Chem., 6 (1967) 369.
28 R. Hoffmann, Science, 211 (1981) 995, and ref. therein.
29 R. Hoffmann and W.N. Lipscomb, J. Chem. Phys., 36 (1962) 2179.
30 Whilst this work was in progress: J.W.A. van der Velden, J.J. Bour and J.J. Steggerda have synthesized $[Au_6(dppe)_4](NO_3)_2$ and shown it to have the structure calculated for $[Au_6(PH_3)_6]^{2+}$ (Inorg. Chem., in press).